On the effects of double-step anneal treatments on light emission from Er-doped Si-rich silicon oxide

C. L. Heng,[a] O. H. Y. Zalloum, J. Wojcik, T. Roschuk, and P. Mascher[b]
Department of Engineering Physics and Centre for Emerging Device Technologies, McMaster University, Hamilton, Ontario L8S 4K1, Canada

(Received 7 September 2007; accepted 7 November 2007; published online 25 January 2008)

We have studied photoluminescence (PL) from an Er-doped Si-rich Si oxide (SRSO) film thermally annealed under different conditions. Compared to the case of annealing in N_2 alone, double-step annealing the film at 875 °C in N_2 and then at ~850 °C in O_2 or vice versa increases Er PL intensities by 10%–15%; while double-step annealing in $N_2+5\%H_2$ (FG) and then in O_2 or vice versa yields significant enhancements of the PL from the SRSO matrix and the Er PL intensity decreases differently by exchanging the processing order. Fourier transform infrared spectroscopy indicates that silicon oxynitride forms after annealing in FG ambient, and for the samples initially oxidized, the increase of Er PL intensity after secondary annealing in N_2 (or FG) is due to more Si nanoclusters being formed. The PL spectra exhibit different annealing behavior with increasing the FG annealing temperature and the processing order. Weak oxygen bonds and silicon oxynitrides are believed to form upon O_2 and FG annealing, respectively, and play important roles in the PL.
 [DOI: 10.1063/1.2829809]

I. INTRODUCTION

During the past decade, Er^{3+} photoluminescence (PL) at 1.54 μm from Er-doped Si-rich Si oxide (SRSO) films has been studied intensively for the development of light sources or small-size and Si-compatible optical amplifiers.[1,2] The excitation of Er^{3+} in the films is usually regarded as originating from the recombination of photogenerated excitons within Si nanoclusters (Si-ncls) and subsequent energy transfer to the nearby Er ions. The efficiency of Er PL depends on the details of Si-ncls (density and size) and Er ions (concentration, distribution, and chemical environment), both of which are strongly dependent on postdeposition annealing conditions for a film with given composition.[3–5] The coupling between Si-ncls and Er dopants usually produces an overall quenching of the intrinsic PL from the SRSO matrix. It has been reported that besides Si-ncls, defects due to excess Si in the SRSO matrix can also act as sensitizers for the Er^{3+} excitation.[6] Thus, investigation of the luminescence from the SRSO matrix can be helpful to reveal further details of the energy transfer mechanism and to find optimized conditions to enhance the emissions from the SRSO matrix on the condition that the Er PL remains efficient, since undoped SRSO has been demonstrated to be an efficient luminescent material.[7,8] This may have potential applications (for example, as light source) in optical integration schemes.

The luminescent properties of undoped SRSO under different annealing conditions have been studied intensively. Wilkinson and Elliman[9] studied the effects of annealing environments [Ar, N_2 or N_2+H_2 (FG)] on the PL from Si nanocrystals (Si-NCs) in silica and attributed the effects to variations in both nanocrystal size and defect states at Si-NC/oxide interface. Comedi *et al.*[10] observed that the PL at long wavelengths can be enhanced greatly by annealing SRSO films in an $Ar+5\%H_2$ ambient and suggested that hydrogen passivating nonradiative recombination centers were responsible for the enhancement. Wolkin *et al.*[11] investigated room temperature oxidation of Si-ncls in a porous Si matrix and suggested that Si=O bonds formed at the SiO_2/Si-ncl interface are crucial to the electronic states and PL of Si-ncls with sizes less than 3 nm. There are also a few reports on the luminescence from Er-doped SRSO after different annealing treatments. Gourbilleau *et al.*[12] annealed Er-doped SRSO films in N_2 and FG, respectively, and suggested that hydrogen passivating dangling bonds were responsible for their Er PL difference. Pi *et al.*[13] studied the formation and oxidation of Si-ncls in Er-doped SRSO films and their effects on the Er PL and gave a kinetic model for the cluster formation and oxidation. We have reported the effects of annealing ambients and double-step annealing treatments on the luminescence of an Er-doped SRSO film.[14] Here, we report the PL anneal behavior of films single treated in N_2 at elevated temperatures and discuss the effects on the PL after different double-step treatments combined with Fourier transform infrared (FTIR) spectroscopy analysis. We also demonstrate how the PL spectra vary with elevated FG anneal temperature when annealing in FG and then in O_2 or vice versa.

II. EXPERIMENTAL DETAILS

The Er-doped SRSO film of 56 nm thickness was synthesized on a single crystal Si substrate by using electron cyclotron resonance plasma-enhanced-chemical-vapor deposition, with an organic Er source supplying the *in situ* doping. Silane and O_2 were used as the precursors to form the SRSO matrix. The deposition conditions have been described in detail elsewhere.[14] Rutherford backscattering spectroscopy analysis yields a Si concentration in the film of 44.7 at. %, with an Er concentration of 1.2 at. %. The film with the sub-

[a]Electronic mail: hengche@mcmaster.ca.
[b]Electronic mail: mascher@mcmaster.ca.

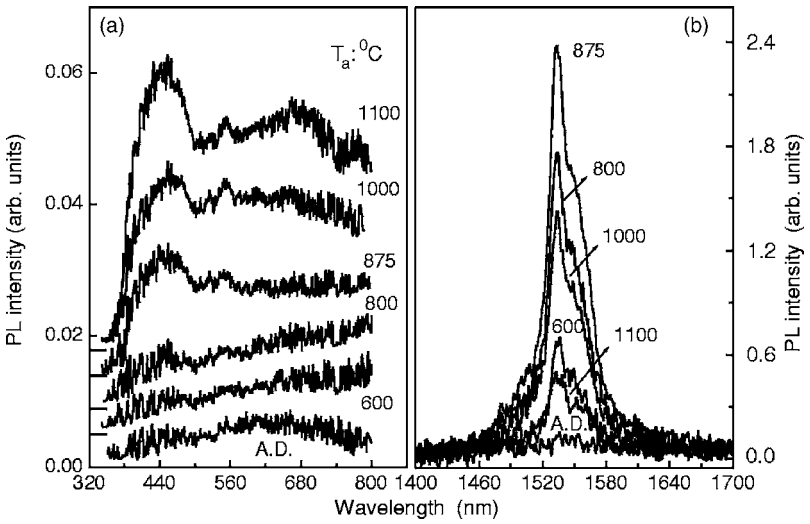

FIG. 1. The PL spectra for the samples AD or annealed in N_2 for 30 min at elevated temperatures (T_a) of 600, 800, 875, 1000, and 1100 °C, respectively: (a) the spectra in the range of 350–800 nm indicative of the emission from the SRSO matrix of the film and (b) the Er^{3+} 1.54 μm PL.

strate was then cleaved into small pieces and subjected to thermal treatments under various conditions. Some samples were single annealed in ultrahigh purity N_2 (99.9999%) for 30 min at 600, 800, 875, 1000, and 1100 °C, respectively; or annealed at 875 °C (or 1100 °C) for 1 h in N_2, FG (N_2 with 5% H_2) and O_2, respectively. Others were subjected to double-step treatments by annealing in N_2 (or FG) for 1 h and then oxidizing at 850 °C for 1 h; or oxidizing at 875 °C for 1 h and then annealing in N_2 (or FG) for 1 h, at the temperatures indicated in text.

The precipitation of Si-ncls was observed with transmission electron microcopy (TEM). The microscope used was a JEOL 2010F field emission gun transmission electron microscope operating at 200 kV. FTIR spectroscopy was used to study the structural changes in such annealed samples by employing a Bio-Rad FTS-40 instrument with a resolution of 4 cm^{-1}. The PL was excited with an unfocused beam (~1 mm diameter) using the 325 nm line of a He–Cd laser with a nominal power of 17 mW. The PL spectra in the 1400–1700 nm range were measured using a 500 mm grating monochromator (3 mm slits), a lock-in amplifier with a chopper working at 40 Hz, and an InGaAs detector. The system response curve for the monochromator is flat over the bandwidth of the Er signal near 1540 nm and therefore, the spectra do not require further correction. The PL spectra in the 350–850 nm range were measured using a charge coupled device (CCD)-based spectrometer. These PL spectra were corrected for system response and optics transmission and subsequently converted to, and presented in normalized photon flux (arbitrary units). A full description of the CCD-based PL system and the data correction methodology are given elsewhere.[15] All the measurements were performed at room temperature.

III. RESULTS AND DISCUSSION

A. Influence of annealing temperature

Figure 1(a) shows the PL spectra of the samples as deposited (AD) or annealed in N_2 for 30 min at the temperatures indicated. The wavelength range from 350 to 800 nm is indicative of luminescence from the SRSO matrix of the film. It can be seen that the PL from the AD sample is very weak. After annealing at 600 °C, the emission at longer wavelengths of the spectrum increases significantly. The PL spectrum becomes more structured as the annealing temperature increases to 800 °C, with two emission bands present in the spectrum with peak positions at 440–450 and 520–550 nm, respectively, and the longer wavelength emission becomes more evident. After an 875 °C annealing, the 440–450 nm band nearly doubles in intensity and becomes the main peak in the spectrum. A small peak near 550 nm clearly appears in the 520–550 nm band. Increasing the annealing temperature further to 1000 and then to 1100 °C, the PL intensity further increases, both the violet-blue band and the 550 nm band become more evident, and the longer wavelength emission yields a peak position at around ~680 nm. Note that the peak positions of the violet-blue band and the 550 nm bands vary little with increasing the annealing temperatures. The origin of the 440–450 nm band can be attributed to some oxygen deficiency centers (ODCs) which are often considered as being responsible for short-wavelength PL in the SRSO films.[16] The 550 nm peak is believed to originate from the transition between Er^{3+} excited states and the ground state ($^4S_{3/2} \rightarrow {}^4I_{15/2}$).[17] The band around 660 nm is normally regarded to originate from nonbridging oxygen hole centers (NBOHCs) in SiO_2.[18,19] In general, the monotonic enhancement of the spectrum intensity can be related to the precipitation of Si-ncls and the decrease of nonradiative recombination with increasing annealing temperature. Also note that the 550 nm peak is still evident after the 1100 °C annealing. This indicates that the size of Si-ncls remains small enough to excite the Er^{3+} to high energy level states consistent with quantum confinement effects.

Figure 1(b) shows the Er PL spectra at ~1.54 μm for the above annealed samples. The Er PL observed from the AD sample is also very weak. This means that the direct excitation of Er^{3+} by the nonresonant laser line is very low. After annealing the sample at 600 °C for 30 min, the Er PL intensity increases evidently. Combined with the fact that the longer wavelength emission was enhanced significantly after the 600 °C annealing, we believe that Si-ncls have precipitated and acted as sensitizers for the Er^{3+} excitation. The PL

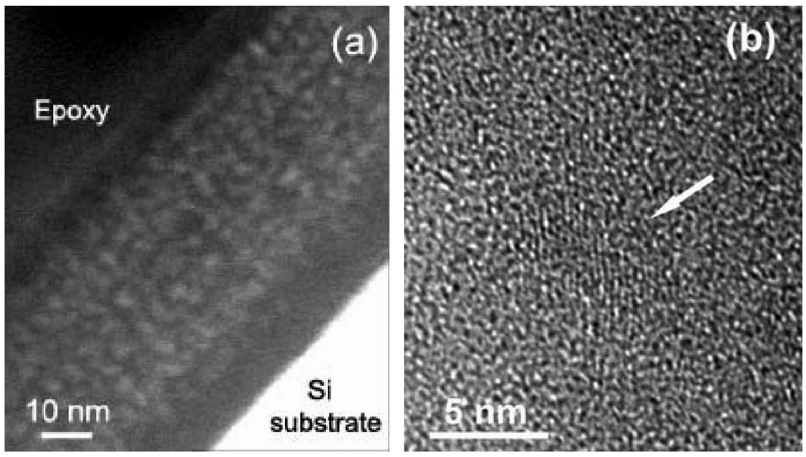

FIG. 2. The precipitation of Si-ncls: (a) EFTEM image for the film after annealing at 875 °C in N_2 for 30 min; (b) HRTEM picture shows Si-NCs have formed after annealing at 1100 °C in N_2 for 30 min.

intensity then increases monotonically and reaches a maximum value after 875 °C anneal and saturates until 900 °C. After that, the Er PL decreases quickly with the anneal temperature increasing further to 1100 °C; and after the 1100 °C annealing, the Er PL intensity is only 20% of the maximum value. We believe that the Er PL annealing behavior is closely related to the precipitations of Si-ncls and Er^{3+} ions in the film. Polman *et al.*[20] have reported similar Er PL annealing behavior for Er-doped thermally grown SiO_2 films; by combining their results with PL lifetime measurements, they attributed the increase of the Er PL intensity mainly to an increment in the luminescence quantum efficiency and a decrease of the PL to the precipitation of Er. It has been demonstrated that the concentration of excited Er ions is proportional to the amount of Si-ncls in Er-doped SRSO;[21] by increasing the annealing temperature, the density of Si-ncls will reach a maximum value at a certain temperature, it then decreases with further increases of the temperature due to the growth of Si-ncls;[13,22] Moreover, the precipitated Si-ncls can act as nucleation centers; the Er distributed around Si-ncls will be clustering and precipitate upon annealing especially at high temperatures (>1000 °C). As such, the Er PL annealing behavior can be readily understood.

B. TEM study

Figure 2(a) shows an energy filtered TEM (EFTEM) picture for the sample annealed at 875 °C in N_2 for 30 min. The image was taken with 3 eV slit in the Si plasmon region (16–19 eV). The white dots are Si-ncls having an average size of about 3–4 nm. Note that the size is a little larger than that reported in a SRSO film with similar Si concentration.[23] We believe that this is due to the Er dopants beneficial to the nucleation and growth of the Si clusters. Figure 2(b) shows a high-resolution TEM picture for the sample annealed at 1100 °C in N_2 for 30 min. Si-NCs are observed to have formed with clear lattice fringes. The Si-NCs increase in size to be about 5 nm but with clearly decreased density compared to the case of 875 °C annealing.

C. PL after single-step annealing at 875 °C in N_2 (or O_2) or double-step treatments combining the two ambients

Besides the anneal temperature, anneal gas ambients have also significant effects on the PL. Figure 3 show the PL spectra for the samples after annealing at 875 °C in N_2, O_2, or double-step treatments combining the two ambients. Each anneal duration has been extended from 30 min to 1 h to further manifest the effects of gas ambients. In Fig. 3(a), for

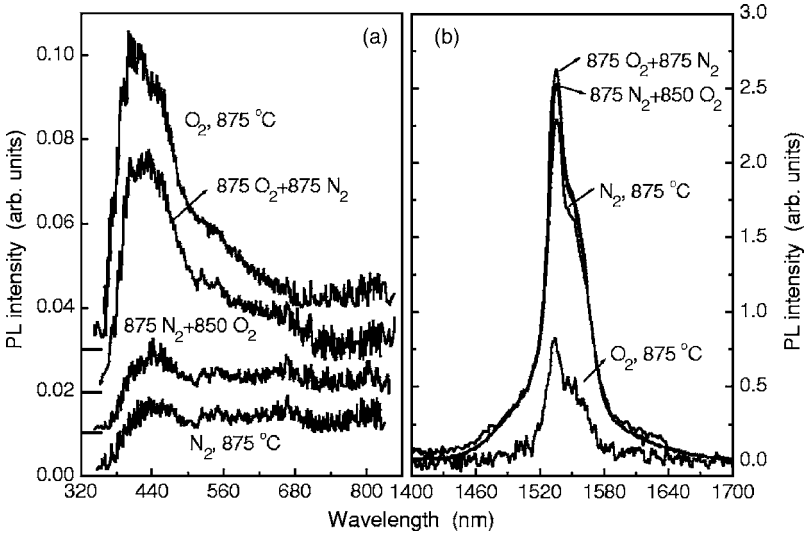

FIG. 3. PL spectra of the samples annealed at 875 °C for 1 h in N_2 and O_2, respectively, or subjected to double-step treatments in 875 N_2+850 O_2 or 875 O_2 +875 N_2: (a) from the SRSO matrix and (b) the Er^{3+} 1.54 μm PL.

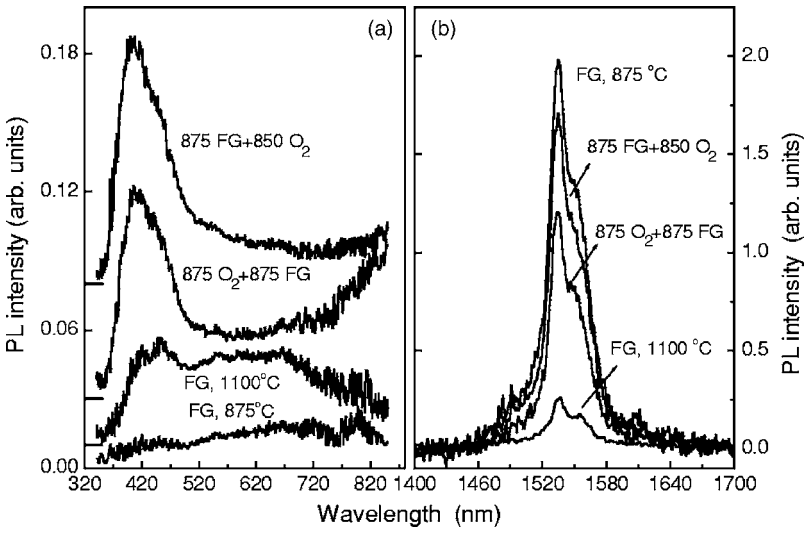

FIG. 4. PL spectra of the samples annealed in FG for 1 h at 875 and 1100 °C, respectively, or subjected to double-step processes of 875 FG+850 O_2 or 875 O_2 +875 FG: (a) from the SRSO matrix and (b) the Er^{3+} 1.54 μm PL.

the sample annealed in N_2 for 1 h, the PL spectrum of the SRSO matrix is similar to that when annealed at the same temperature but for 30 min; while after annealing in O_2, the PL intensity increases significantly, a ~405 nm band emerges in the spectrum and becomes the dominant peak, the 440–450 nm band is still present but as a shoulder, and the emission with wavelengths longer than 660 nm decreases significantly. We believe that Si-ncls have also precipitated after the 875 °C oxidation, but the amount of the clusters is smaller than that in the N_2 annealing case and a very thin oxide layer likely surrounds each Si-ncl.[13] The 405 nm band has been attributed to localized surface states at the SiO_x/Si interface after oxidizing Si-NCs,[24] and we suggest that the surface states could be weak oxygen bonds (WOBs).[25] Even though no interstitial O atoms were generated as through Si ion implantation,[26] O atoms can diffuse into the film upon oxidation to form WOB defects at the surface of Si-ncls.

Since oxidization significantly enhances the violet-blue emission of the film, we have treated samples by combining the oxidation with the N_2 annealing, also shown in Fig. 3(a). It can be seen that after annealing the sample in N_2 and then oxidizing at 850 °C (875 N_2+850 O_2), the PL spectrum is similar to the case of annealing in N_2 alone, secondary oxidation seems to have little effect on the PL; however, for the sample initially oxidized at 875 °C and then annealed at 875 °C in N_2 (875 O_2+875 N_2), the PL intensity decreased by ~23% compared to the case of oxidation alone. For the 875 N_2+850 O_2 treatments, the small variation of the PL spectrum after secondary oxidation suggests that the oxidation of Si-ncls should be slight or be a self-limiting process as in the Si-NC case;[27] while for the 875 O_2+875 N_2 treatments, the small decrease in PL intensity after secondary annealing in N_2 is likely due to the initially formed WOB defects being partially reduced.

Figure 3(b) shows the Er PL spectra for the above samples. After annealing the sample at 875 °C in N_2 for 1 h, the PL intensity decreases slightly (~4%) compared to the case of annealing in N_2 but for 30 min. However, after annealing in O_2 the intensity is only 37% of that annealed in N_2 under identical conditions. The strong decrease in intensity is due either to fewer Si-ncls formed or a decrease of "effective" Si-ncl size after the oxidation.[13] In the case of double-step annealing in 875 N_2+850 O_2, the Er PL intensity is about 10% stronger than in the case of annealing in N_2 alone. This is possibly due to the size of Si-ncls being decreased slightly after the secondary oxidation which improves the quantum excitation efficiency by reducing the energy back transfer from Er^{3+} ions to Si-ncls.[17] For the 875 O_2 +875 N_2 treatments, the Er PL intensity has increased by about a factor of 2 compared to the case of oxidation alone, and it is also about 15% stronger when compared to the case of annealing in N_2 alone. The pronounced enhancement is attributed to either the amount of the Si-ncls or the effective Si-ncl size being greatly increased. Note that the intensities for the above two double-step anneal cases are almost identical despite the processing order. If the concentration of optically excited Er ions is proportional to the number of Si-ncls in Er-doped SRSO, then the number of Si-ncls formed in the film after these two double-step treatments should be almost the same.

D. PL after single annealing in FG at 875 °C (or 1100 °C) or double-step treatments of combining the FG and O_2 annealing

N_2 is believed to be relatively inert for annealing temperatures less than 1200 °C, however, N_2 can react with Si to form ultrathin silicon oxynitride near the Si/SiO_2 interface at moderate temperatures (760–1050 °C) in the presence of gas impurities (H_2, O_2, CO_2).[28] We believe that silicon oxynitrides, with PL emission at wavelengths around ~430 nm,[29] have been formed on the surface of Si-ncls upon annealing our film in FG.[14] The formation of silicon oxynitrides has significant effects on the PL from both the SRSO matrix and the Er^{3+} ions, as is shown in Figs. 4(a) and 4(b), respectively. In Fig. 4(a), when annealing the sample at 875 °C in FG for 1 h, the 440–450 nm band in the PL spectrum becomes weaker, while the 660 and 800 nm emissions are slightly stronger than those in the case of annealing in N_2. The decrease of the blue band is due to the formation of silicon oxynitride at the expense of ODC defects, but the amount of the oxynitrides is so small that it cannot be re-

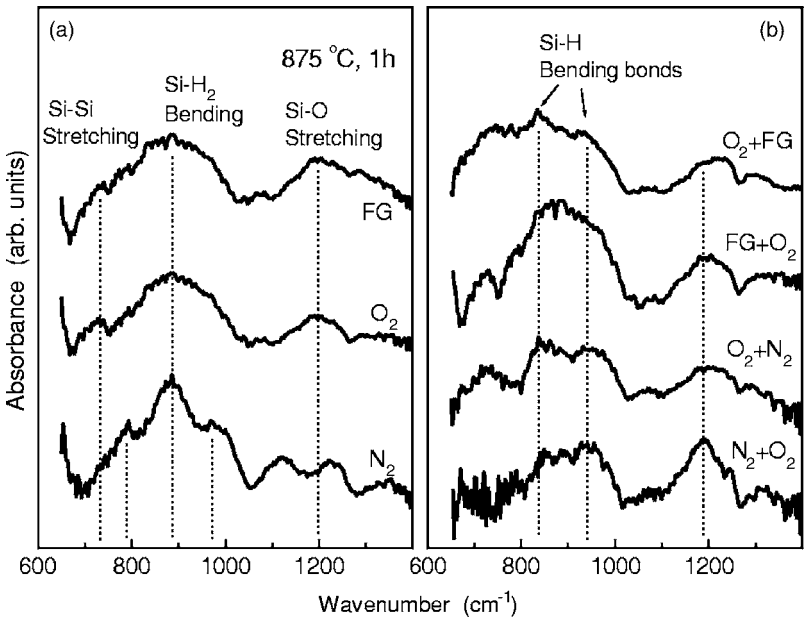

FIG. 5. FTIR spectra of the samples (a) after single-step annealing at 875 °C for 1 h in N_2, O_2, and FG, respectively; (b) after different double-step processes of 875 N_2+850 O_2, 875 O_2+875 N_2, 875 FG+850 O_2, and 875 O_2+875 FG.

flected in the spectrum.[14] The emissions at around 800 nm or longer are normally regarded as originating from the radiative recombination within Si-ncls;[30] and the stronger 660 and 800 nm bands are due to hydrogen passivating nonradiative recombination centers.[10,14] After annealing at 1100 °C in FG, the PL intensity clearly increases; there seem to be two structures present in the violet-blue band with peak positions at around ~420 and ~450 nm, respectively; the ~680 nm band is also stronger than that in the case of 1100 °C N_2 annealing. The appearance of the 420 nm peak indicates that more oxynitrides have formed after the 1100 °C FG annealing. It should be noted that for the sample annealed at 1100 °C in O_2, the PL intensity is about twice as strong as that in the case of 875 °C oxidation.

Figure 4(a) also shows the PL spectra for the samples after double-step treatments in FG and then in O_2 or vice versa. For the sample annealed at 875 °C in FG and then oxidized at 850 °C (i.e., 875 FG+850 O_2), the spectrum has a major peak at around 405 nm, the intensity is about nine times stronger than that in the case of annealing in FG alone, but the 660 nm and the 820 nm bands remain weak. The significant enhancement of the intensity should be related to the introduction of defects (silicon oxynitrides and WOB) through the double-step treatments. For the sample initially oxidized at 875 °C and then annealed at 875 °C (i.e., 875 O_2+875 FG), the PL intensity is only 25% more intense than that in the case of 875 °C oxidation alone, but the 660 nm band, and especially the 820 nm band are observed to be greatly enhanced. The evident increase of the 660 nm band after secondary FG annealing is believed to be due to the H_2 passivation being beneficial to the formation of NBOHC possibly by breaking the weak O–O bonds, with WOB being the precursor of NBOHC in our film.[14,31] The significant enhancement of the 820 nm band should also be due to the formation of silicon oxynitrides which hinders the energy transfer from Si-ncls to Er ions, thus increasing greatly the radiative recombination within Si-ncls.

Figure 4(b) shows the corresponding Er PL spectra for the above annealed samples. Compared to the case of annealing in N_2, after annealing the sample at 875 °C in FG, the PL intensity has decreased by ~10%; and after annealing at 1100 °C in FG, the intensity decreases drastically to be only 13% of the original. For double-step treatments of 875 FG +850 O_2, the PL intensity has decreased by ~14% after the secondary oxidation. This intensity is also lower than that in the case of 875 N_2+850 O_2 treatments. The decrease of the Er PL should be closely related to the formation of silicon oxynitrides at the surface of Si-ncls that partly hinders the energy transfer. This will be discussed further in Secs. III E and III F. Note that after the 875 O_2+875 FG treatments, the Er PL intensity has increased by 50% when compared to the case of 875 °C oxidation alone, but decreases to be 60% of the original if compared to the case of 875 °C FG annealing. The intensity is also much lower than that in the case of 875 O_2+875 N_2 treatments, which again demonstrates the influence of the oxynitride.

E. FTIR study

The structural changes in the samples after the above single- and double-step annealing processes were investigated by FTIR spectroscopy. Figures 5(a) and 5(b) show the spectra of the samples in a range of 650–1400 cm^{-1}. In Fig. 5(a), for the sample annealed at 875 °C in N_2, there are five absorption bands including shoulders present in the spectrum with peak positions at around 793, 886, 970, 1120, and 1225 cm^{-1}, respectively. Since silane was used as the precursor in the deposition, it is not unexpected to have $Si–H_x$ (x=1,2) bonds in the film. The 793 cm^{-1} peak can be assigned to a certain Si–H bending vibration with local-bonding configuration of $HSi–Si_2O$.[32,33] The 886 cm^{-1} peak is normally attributed to $Si–H_2$ bending vibrations.[34–36] Another type of Si–H group with local configuration of $H_2Si–O_2$ has been ascribed to be responsible for the absorption at ~976 cm^{-1};[33,37] our 970 cm^{-1} shoulder is possibly

from the Si–H bending mode. The two small absorption bands at around 1120 and 1225 cm^{-1} are believed to come from out-of-phase (or "asymmetric") Si–O stretching vibrations.[38,39] After the 875 °C oxidation, an absorption peak at around 730 cm^{-1} emerges in the spectrum which is possibly related to certain Si–Si stretching vibrations;[38,40] the main 886 cm^{-1} peak decreases in intensity and broadens evidently, and the 970 cm^{-1} peak smears out into the main band. The variations in the peaks are believed to be due to oxidation of the film causing the dissociation of Si-H_x bonds to form Si–Si and/or Si–H bonds, as has been observed for oxidation of porous Si.[37] Note that after the oxidation treatment only one absorption band appears at around 1200 cm^{-1}. For the sample annealed at 875 °C in FG the main 886 cm^{-1} band and the absorption peak at ~1200 cm^{-1} are wider than those in the cases of N_2 (or O_2) annealing. Besides the $Si-H_2$ bonds being dissociated, we believe that the broadening of the peaks is also due to the formation of Si–N (possibly by $Si-Si+N-H \rightarrow Si-H+Si-N$) (Ref. 41) and/or Si–O–N bonds[42] upon the FG annealing, since Si–N stretching modes can have wide absorption from 734 to 904 cm^{-1} (Refs. 43 and 44). This is consistent with the assumption of silicon oxynitride formation as suggested from the PL measurements.

In Fig. 5(b), for the sample after double-step treatments of 875 N_2+850 O_2, the 793 cm^{-1} peak becomes less evident in the spectrum when compared to the case of 875 °C annealing in N_2 alone, the main 886 cm^{-1} peak decreases much in intensity and two additional absorption peaks emerge at around 848 and 939 cm^{-1}, respectively. The 848 cm^{-1} shoulder can also be ascribed to certain Si–H bonds with local configuration of $HSi-SiO_2$,[37] and the 939 cm^{-1} band is reported to have the same origin as the 976 cm^{-1} shoulder.[33] Therefore, the variations in the peaks can be due to the $Si-H_2$ bonds being oxidized and certain Si–H bonds being formed. Note that after the secondary oxidation, only one major peak appears in the spectrum with peak position at around 1190 cm^{-1}. From this, combined with the observations for the single N_2 (or O_2) annealing cases, we believe that the oxidation has changed the "symmetry" of the Si–O bonds. Under the reverse 875 O_2+875 N_2 treatments, compared to the case of 875 °C oxidation alone, the 730 cm^{-1} band increases in intensity and broadens after the secondary N_2 annealing, which indicates more Si-ncls have precipitated. Hence, the fact that the Er PL shows two times enhancement can be understood. The 886 cm^{-1} peak decreases in intensity and two bands (~837 and ~945 cm^{-1}) appear in the spectrum, which are ascribed to the dissociation of $Si-H_2$ bonds upon the secondary N_2 annealing. On the other hand, for the sample after double-step treatments in 875 FG+850 O_2, the main 886 cm^{-1} peak and especially the 1200 cm^{-1} peak becomes narrower when compared to the case of 875 °C FG annealing alone. It has been suggested that the incorporation of N into the Si/SiO_2 interface is not chemically stable;[28] the narrowing of the peaks is likely due to the Si–O–N bonds formed upon the FG annealing being replaced by Si–O bonds upon the secondary oxidation. After the 875 O_2+875 FG treatments, the intensity of the 733 cm^{-1} peak increases compared to the 875 °C oxidation alone which indicates that more Si-ncls have formed. This can explain the 50% increase of the Er PL after secondary FG annealing. Note that two bands appear in the spectrum with peak positions at 833 and 928 cm^{-1}, respectively, which is again attributed to the dissociation of $Si-H_2$ bonds into Si–H bonds.

F. Influences of FG annealing temperature and processing order

From the above measurements, silicon oxynitrides are believed to form around Si-ncls upon annealing in FG, and the amount increases with increasing annealing temperature. Double-step annealing in FG and then in O_2 or vice versa yields different final oxides at the surface of Si-ncls, which affects the PL from the SRSO matrix (mainly Si-ncls) and thus from the Er^{3+} ions. Figure 6 shows how the PL spectra of the samples vary as a function of the FG annealing temperature and the processing order in the double-step treatments of annealing in FG and then in O_2 or vice versa. In Fig. 6(a), for the sample initially annealed at 950 °C in FG followed by 850 °C oxidation (950 FG+850 O_2), the PL from the SRSO matrix decreases in intensity, and the peak position of the violet-blue band redshifts from 404 to 435 nm compared to the case of 875 FG+850 O_2 treatments. As the FG annealing temperature increases further to 1000 and then to 1050 °C, the intensity of the violet-blue band increases slowly, but the emissions at longer wavelengths (>650 nm) are evidently enhanced. After 1100 °C annealing in FG and then in 850 °C oxidation (1100 FG +850 O_2), both the violet-blue band and the longer emission band increase significantly in intensity; the peak position of the violet-blue band shifts back to 419 nm and the longer emission band has an evident peak position at ~820 nm.

Green *et al.*[28] have suggested that upon double-step treatments of rapid thermal nitriding and then rapid thermal oxidizing of a clean Si wafer, as the preincorporated N content is less than 10^{15} N at./cm^2, the lower the N content, the thicker the final oxide thickness on the Si surface after the secondary oxidation. If, however, the N content is higher than 10^{15} N at./cm^2, the final oxide thickness tends to saturate with increasing N content. Similar phenomena appear to have occurred in our case as the FG annealing temperature increases from 875 to 1050 °C. Compared to the case of 875 FG+850 O_2 treatments, after 950 °C FG annealing more silicon oxynitride forms, and the N content increases; then less final oxide is formed around the Si-ncls after the secondary 850 °C oxidation. Hence, the decrease of the intensity of the violet-blue band can be understood. Also due to more oxynitride being formed, the radiative recombination within Si-ncls increases, the intensity of the 820 nm band starts to increase. As the FG annealing temperature increases to 1000 and then to 1050 °C, even more oxynitride forms, and the N content in the oxynitride may become higher than ~10^{15} N at./cm^2. After secondary oxidation the final oxide around Si-ncls seems to saturate, and the PL intensities of the violet-blue band and the 820 nm band are nearly identical in both cases. However, the significant increases of the violet-blue band and the 820 nm band after the 1100 FG+850 O_2

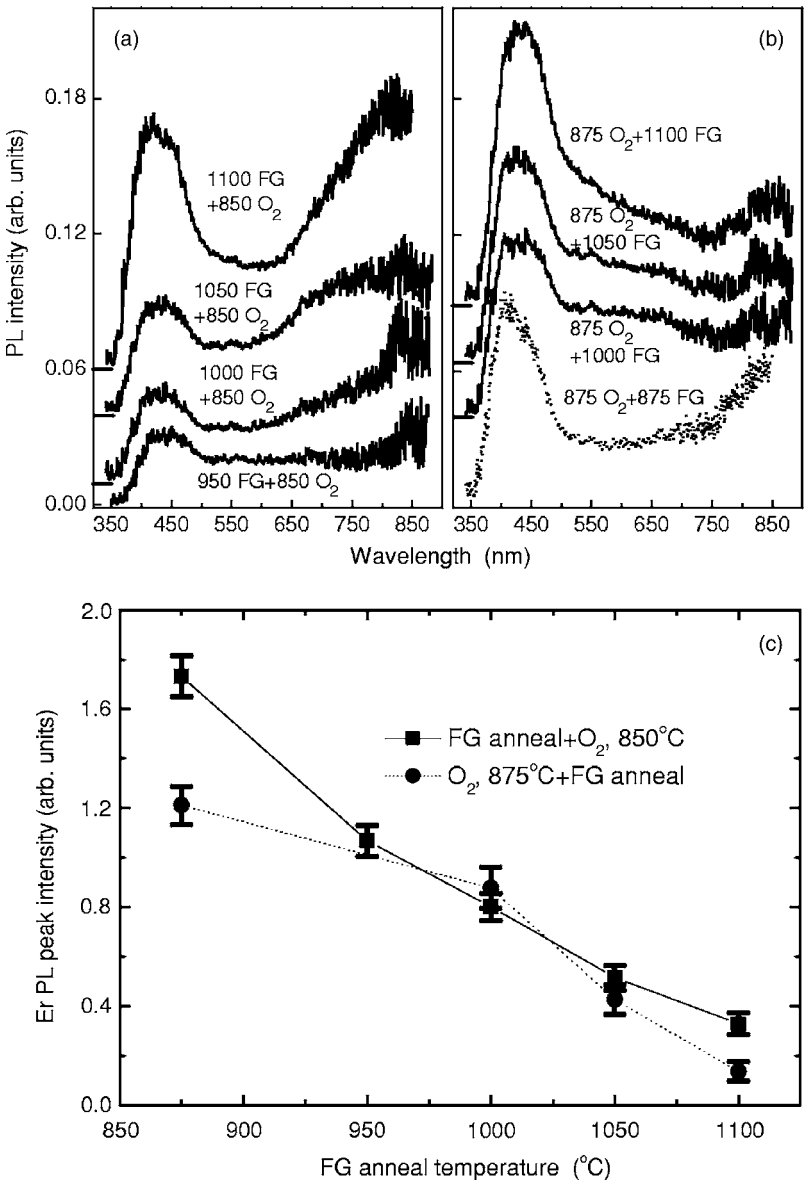

FIG. 6. (a) The PL from the SRSO matrix of the samples after double-step processes of annealing in FG and then in O_2. The FG anneal temperature varies from 950 to 1100 °C and the oxidation temperature is kept at 850 °C. (b) The PL from the SRSO matrix of the samples after double-step processes of oxidizing at 875 °C and then annealing in FG. The oxidation temperature is kept at 875 °C, while the secondary FG anneal temperature increases from 875 to 1100 °C. (c) The Er PL peak intensities of spectra for the samples after the above double-step treatments.

treatments indicate that the final oxide around the Si-ncls actually continues to increase rather than saturate. The gradual increase of the 650–800 nm emission is believed to be due to the passivating capability of hydrogen increasing with elevated FG annealing temperature.[45]

By exchanging the processing order, the PL from the SRSO matrix of the film exhibits different annealing behavior with increasing the FG annealing temperature, as is shown in Fig. 6(b). For the sample oxidized at 875 °C and then annealed at 1000 °C in FG (875 O_2+1000 FG), compared to the case of 875 O_2+875 FG treatments (plotted as a dotted line), the violet-blue band decreases in intensity but becomes wider and seems to contain small structures; the emissions in the range of 500–700 nm are enhanced, while the 820 nm band decreases substantially in the PL spectrum. The variation of the violet-blue band is possibly due to the WOB defects being significantly reduced but the formation of silicon-oxynitride not being able to make up for the decrease. The enhancement of the 500–700 nm emission is related to the formation of NBOHC from the reduction of the WOB defects. Since the oxide around Si-ncls has been much reduced, the radiative recombination within Si-ncls decreases greatly and the 820 nm band decreases much in intensity. With increasing the FG annealing temperature to 1050 °C (i.e., 875 O_2+1050 FG) and then to 1100 °C (i.e., 875 O_2 +1100 FG), the violet-blue band increases continuously in intensity, its peak position shifts to 425 and then to 433 nm; the 550–750 nm emission decreases slightly, while the 820 nm band increases a little. The increases of the intensity of the violet-blue band and the shifts of the peak position are likely due to more oxynitride being generated with increasing the FG annealing temperature. However, the fact that the 820 nm band shows no significant enhancement indicates that the amount of final Si oxide is still not large enough to affect the radiative recombination within Si-ncls. The increase of the spectrum intensity is also possible due to the decrease of nonradiative recombination with increasing the FG annealing temperature.

Figure 6(c) shows the PL peak intensities of the Er PL spectra for the samples after the above double-step processes. For the samples initially annealed in FG and then subjected to an 850 °C oxidation, with increasing the FG

annealing temperature from 875 to 950 °C, the Er PL intensity has decreased to 60%; as the temperature increases further to 1100 °C, the intensity decreases drastically to be only 19% after the secondary oxidation. For the samples initially oxidized at 875 °C, with increasing the secondary FG annealing temperature from 875 to 1000 °C, the Er PL intensity decreases to be 70%, and decreases to be only 11% as the temperature increases to 1100 °C. Comparing the two Er PL intensity curves, we find that the samples which were subjected to FG annealing and then to oxidation generally have stronger intensity than those initially oxidized and then subjected to FG annealing treatments. The reasons for this phenomenon are not entirely clear at this time. However, from the Er PL intensity of the sample single annealed at 875 °C in FG being much stronger than that from the sample annealed at the same temperature in O_2, we believe that more Si-ncls have formed upon FG annealing than in O_2 annealing. The environment of Er^{3+} ions after double-step treatments could also play an important role in the observed differences in the Er PL. It appears that a secondary 850 °C oxidation is favorable for the Er^{3+} to be in an efficient state for the Er PL. This is supported by the observation that the Er PL for the sample after the 1100 FG+850 O_2 treatments is 25% stronger than that after the 1100 °C FG annealing alone.

From Figs. 3, 4, and 6, it can be seen that the annealing procedure (1100 FG+850 O_2) is most beneficial for the PL efficiency from the SRSO matrix, since the integrated PL intensity is much stronger than those under the other treatments; while double-step treatments of 875 O_2+875 N_2 yields the highest Er PL among all the annealing procedures. It is noted, however, that most of the annealing procedures at or near 875 °C have not significantly influenced the final PL efficiency from Er^{3+} ions, the Er PL shows only 1.5–2.2 times increases in intensity.

IV. CONCLUSIONS

We have studied the PL from an Er-doped SRSO film with samples annealed under different conditions. For the samples annealed in N_2 alone, the PL intensity of the SRSO matrix increases monotonically with increasing the annealing temperature, while the Er PL reaches a maximum intensity upon an 875 °C annealing. Double-step annealing in N_2 and then in O_2 or vice versa yields higher Er PL intensities than those from the samples annealed in FG and then in O_2 or vice versa. The 1100 FG+850 O_2 treatment seems most beneficial for the PL from the SRSO matrix. FTIR analysis indicates that for the samples initially oxidized, the enhancements of Er PL after secondary annealing in N_2 (or FG) are due to more Si-ncls being formed; the broadening of the absorption peaks is due to Si–H_2 bonds being dissociated into Si–H bonds and the formation of Si–N and/or Si–O–N bonds upon the FG annealing. The final oxides around Si-ncls (both WOB defects and silicon oxynitride) vary with increasing the FG annealing temperature and the processing order upon double-step treatments in FG and then in O_2 or vice versa. The control of light emission from Er-doped SRSO matrix by double-step treatments may have important applications in solid state lighting and chip-to-fiber communication in integrated optoelectronic devices.

ACKNOWLEDGMENTS

The authors wish to acknowledge valuable technical support by Jim Garrett during the annealing experiments. This work has been supported by the Ontario Research and Development Challenge Fund under the auspices of the Ontario Photonics Consortium.

[1] A. J. Kenyon, P. F. Trwoga, M. Federighi, and C. W. Pitt, J. Phys.: Condens. Matter **6**, L319 (1994).
[2] Physica E, Vol. **16**, Issues 3–4 (2003).
[3] G. Franzó, S. Boninelli, D. Pacifici, F. Priolo, F. Iacona, and C. Bongiorno, Appl. Phys. Lett. **82**, 3871 (2003).
[4] C. Y. Chen, W. D. Chen, S. F. Song, Z. J. Xu, X. B. Liao, G. H. Li, and K. Ding, J. Appl. Phys. **94**, 5599 (2003).
[5] A. Janotta, M. Schmidt, R. Janssen, and M. Stutzmann, Phys. Rev. B **68**, 165207 (2003).
[6] D. Kuritsyn, A. Kozanecki, H. Przybylińska, and W. Jantsch, Appl. Phys. Lett. **83**, 4160 (2003).
[7] M. J. A. de Dood, J. Knoester, A. Tip, and A. Polman, Phys. Rev. B **71**, 115102 (2005).
[8] See, for example, *Silicon Photonics*, edited by L. Pavesi and D. J. Lockwood (Springer, Berlin, 2004); R. J. Walters, G. I. Bourianoff, and H. A. Atwater, Nat. Mater. **4**, 143 (2005).
[9] A. R. Wilkinson and R. G. Elliman, J. Appl. Phys. **96**, 4018 (2004).
[10] D. Comedi, O. H. Y. Zalloum, and P. Mascher, Appl. Phys. Lett. **87**, 213110 (2005).
[11] M. V. Wolkin, J. Jorne, P. M. Fauchet, G. Allan, and C. Delerue, Phys. Rev. Lett. **82**, 197 (1998).
[12] F. Gourbilleau, P. Choppinet, C. Dufour, M. Levalois, R. Madelon, J. Vicens, R. Rizk, and M. Prassas, Mater. Sci. Eng., B **105**, 44 (2003).
[13] X. D. Pi, O. H. Y. Zalloum, J. Wojcik, A. P. Knights, P. Mascher, A. D. W. Todd, and P. J. Simpson, J. Appl. Phys. **97**, 096108 (2005).
[14] C. L. Heng, O. H. Y. Zalloum, T. Roschuk, D. Blakie, J. Wojcik, and P. Mascher, Electrochem. Solid-State Lett. **10**, K20 (2007).
[15] O. H. Y. Zalloum, M. Flynn, T. Roschuk, J. Wojcik, E. Irving, and P. Mascher, Rev. Sci. Instrum. **77**, 023907 (2006).
[16] L. Rebohle, J. von Borany, H. Fröb, and W. Skorupa, Appl. Phys. B: Lasers Opt. **71**, 131 (2000).
[17] A. Polman, J. Appl. Phys. **82**, 1 (1997).
[18] A. R. Silin, L. N. Skuja, and A. V. Shendrik, Fiz. Khim. Stekla **4**, 405 (1978).
[19] L. N. Skuja and A. R. Silin, Phys. Status Solidi A **56**, K11 (1979).
[20] A. Polman, D. C. Jacobson, D. J. Eaglesham, R. C. Kistler, and J. M. Poate, J. Appl. Phys. **70**, 3778 (1991).
[21] M. Wojdak, M. F. M. Klik, O. B. Gusev, T. Gregorkiewicz, G. F. D. Pacifici, F. Priolo, and F. Iacona, Phys. Rev. B **69**, 233315 (2004).
[22] F. Gourbilleau, M. Levalois, C. Dufour, J. Vicens, and R. Rizk, J. Appl. Phys. **95**, 3717 (2004).
[23] F. Iacona, C. Bongiorno, C. Spinella, S. Boninelli, and F. Priolo, J. Appl. Phys. **95**, 3723 (2004).
[24] X. Y. Chen, Y. F. Lu, Y. H. Wu, B. J. Cho, M. H. Liu, D. Y. Dai, and W. D. Song, J. Appl. Phys. **93**, 6311 (2003).
[25] J. C. Cheang-Wong, A. Oliver, J. Roiz, J. M. Hernandez, L. Rodrigues-Fernandez, J. G. Morales, and A. Crespo-Sosa, Nucl. Instrum. Methods Phys. Res. B **175-177**, 490 (2001).
[26] G.-R. Lin, C.-J. Lin, C.-K. Lin, L.-J. Chou, and Y.-L. Chueh, J. Appl. Phys. **97**, 094306 (2005).
[27] D. B. Kao, J. P. McVittie, W. D. Nix, and K. C. Saraswat, IEEE Trans. Electron Devices **ED-35**, 25 (1988).
[28] M. L. Green, T. Sorsch, L. C. Feldman, W. N. Lennard, E. P. Gusev, E. Garfunkel, H. C. Lu, and T. Gustafsson, Appl. Phys. Lett. **71**, 2978 (1997).
[29] J. Zhao, Y. H. Yu, D. S. Mao, Z. X. Lin, B. Y. Jiang, G. Q. Yang, X. H. Liu, and Shichang Zou, Nucl. Instrum. Methods Phys. Res. B **148**, 1002 (1999).

[30]M. Fujii, K. Imakita, K. Watanabe, and S. Hayashi, J. Appl. Phys. **95**, 272 (2004).
[31]H. Nishikawa, R. Nakamura, R. Tohmon, Y. Ohki, Y. Sakurai, K. Nagasawa, and Y. Hama, Phys. Rev. B **41**, 7828 (1990).
[32]G. Lucovsky, J. Yang, S. S. Chao, J. E. Tyler, and W. Czubatyj, Phys. Rev. B **29**, 2302 (1984).
[33]D. V. Tsu, G. Lucovsky, and B. N. Davidson, Phys. Rev. B **40**, 1795 (1989).
[34]G. G. Salgado, T. D. Becerril, H. J. Santiesteban, and E. R. Andrés, Opt. Mater. (Amsterdam, Neth.) **29**, 51 (2006).
[35]A. J. Steckl, J. Xu, H. C. Mogul, and S. M. Prokes, J. Electrochem. Soc. **142**, L69 (1995).
[36]D. Comedi, O. H. Y. Zalloum, E. A. Irving, J. Wojcik, and P. Mascher, J. Vac. Sci. Technol. A **24**, 817 (2006).
[37]X.-W. Du, Y.-W. Lu, J.-P. Liu, and J. Sun, Appl. Surf. Sci. **252**, 4161 (2006).
[38]Z. Yu, M. Aceves-Mijares, E. Quiroga, R. Lopez-Estopier, J. Carrillo, and C. Falcony, J. Appl. Phys. **100**, 013524 (2006).
[39]M. I. Alayo, I. Pereyra, W. L. Scopel, and M. C. A. Fantini, Thin Solid Films **402**, 154 (2002).
[40]T. Morioka, S. Kimura, N. Tsuda, C. Kaito, Y. Saito, and C. Koike, Mon. Not. R. Astron. Soc. **299**, 78 (1998).
[41]Y. Xin, Z. X. Huang, Y. Shi, L. Pu, R. Zhang, and Y. D. Zheng, Physica E (Amsterdam) **30**, 41 (2005).
[42]M. Bedjaoui, B. Despax, M. Caumont, and C. Bonafos, Mater. Sci. Eng., B **124–125**, 508 (2005).
[43]S. J. Patil and S. A. Gangal, J. Micromech. Microeng. **15**, 1956 (2005).
[44]Ruofeng Guo, Y. Kurata, T. Inokuma, and S. Hasegawa, J. Non-Cryst. Solids **351**, 3006 (2005).
[45]D. Comedi, O. H. Y. Zalloum, J. Wojcik, and P. Mascher, IEEE J. Sel. Top. Quantum Electron. **12**, 1561 (2006).